Anti-tumor activity of silymarin nanoliposomes in combination with iron: *In vitro* and *in vivo* study

Maham Doagooyan [a,b], Seyedeh Hoda Alavizadeh [c,d], Amirhossein Sahebkar [e,f,**], Kebria Houshangi [b], Zahra Khoddamipour [b], Fatemeh Gheybi [b,c,*]

[a] *Student Research Committee, Mashhad University of Medical Sciences, Mashhad, Iran*
[b] *Department of Medical Biotechnology and Nanotechnology, Faculty of Medicine, Mashhad University of Medical Sciences, Mashhad, Iran*
[c] *Nanotechnology Research Center, Pharmaceutical Technology Institute, Mashhad University of Medical Sciences, Mashhad, Iran*
[d] *Department of Pharmaceutical Nanotechnology, School of Pharmacy, Mashhad University of Medical Sciences, Mashhad, Iran*
[e] *Biotechnology Research Center, Pharmaceutical Technology Institute, Mashhad University of Medical Sciences, Mashhad, Iran*
[f] *Applied Biomedical Research Center, Mashhad University of Medical Sciences, Mashhad, Iran*

A B S T R A C T

Combination therapy represents a promising strategy in cancer management by reducing chemotherapy resistance and associated side effects. Silymarin (SLM) has been extensively investigated due to its potent antioxidant properties and demonstrated efficacy against cancer cells. Under certain conditions however, polyphenolic compounds may also exhibit prooxidant activity by elevating intracellular reactive oxygen species (ROS), which can harm the target cells. In this study, we hypothesized that the simultaneous administration of iron (Fe) could alter the antioxidant characteristic of SLM nanoliposomes (SLM Lip) to a prooxidant state. Hence, we first developed a SLM Lip preparation using lipid film method, and then investigated the anti-oxidant properties as well as the cytotoxicity of the liposomal preparation. We also explored the efficacy of concomitant administration of iron sucrose and SML Lip on the tumor growth and survival of mice bearing tumors. We observed that exposing cells to iron, and consecutive treatment with SLM Lip (Fe + SLM Lip) could induce greater toxicity to 4 T1 breast cancer cells compared to SLM Lip. Further, Fe + SLM Lip combination demonstrated a time-dependent effect on reducing the catalase activity compared to SLM Lip, while iron treatment did not alter cell toxicity and catalase activity. In a mouse breast cancer model, the therapeutic efficacy of Fe + SLM Lip was superior compared to SLM Lip, and the treated animals survived longer. The histopathological findings did not reveal a significant damage to the major organs, whereas the most significant tumor necrosis was evident with Fe + SLM Lip treatment. The outcomes of the present investigation unequivocally underscored the prospective use of Fe + SLM combination in the context of cancer therapy, which warrants further scrutiny.

1. Introduction

The global prevalence of cancer is on the rise, and it is a significant contributor to the reduced life expectancy and premature mortality in 112 nations prior to the age of 70, as reported by the World Health Organization (WHO) in 2020 (Sung et al., 2021). There are a multitude of factors that play a role in the development of cancer, including various lifestyle behaviors including smoking, inadequate dietary habits, and a lack of physical activity (Ferlay et al., 2015). Female breast cancer is now the most frequently diagnosed cancer with approximately

2.3 million new cases (Dorling et al., 2022; Sung et al., 2021), 1 in 4 cancer cases, and 1 in 6 cancer death in the women population (Borri and Granaglia, 2021). Although chemotherapy is commonly considered as the leading therapeutic modality, the occurrence of severe toxic side effects, inadequate targeting of tumor sites, and the development of resistance through genetic alterations in cancer cells all contribute to a reduction in the treatment efficacy (Krohne, 2017; Redd et al., 2021). In light of the aforementioned limitations, combination therapy has become the cornerstone of the therapeutic strategies aimed at mitigating these effects and augmenting therapeutic efficacy. Over the recent years,

considerable attention has been devoted to the role of herbal medicine, particularly in the use of flavonoids and polyphenols, which have demonstrated potential in both curative and complementary cancer therapies (Bernstein and Webster, 2021; Ezzati et al., 2020). Herbal medicines are being used in numerous countries as an efficient and alternative remedy for chronic diseases including cancer (Kwon et al., 2021; Zhang et al., 2020). Numerous drawbacks of herbal medicines have been resolved by the development of nanotechnology (Zhang et al., 2021), including reduced metabolism and degradation (Basak et al., 2021), and improved physicochemical properties including enhanced solubility by using nanocarriers (Bonifacio et al., 2014; Zhao et al., 2019). Nanocarriers possess the potential to surmount biological impediments, thereby aiding the ingress of their therapeutic load into the systemic circulation (Chen et al., 2019; Hashemi Goradel et al., 2018; Li et al., 2014; Sanati et al., 2023).

Silymarin, a derivative of *Silybum marianum*, commonly known as milk thistle, is believed to have originated from the mountainous regions of the Mediterranean, encompassing Europe, North Africa, and the Middle East. Its historical usage in the treatment of diverse liver and gallbladder-related maladies dates back to ancient times (Abenavoli et al., 2010). Silymarin is a mixture of phytochemicals comprising 65–80% flavonolignans including silybin, silychristin, isosilybin silydianin (Deep et al., 2006; Gazak et al., 2007), as well as 20–35% fatty acids and other polyphenolic ingredients (Ramasamy and Agarwal, 2008). Silymarin is known for its antioxidant and pro-apoptotic properties (Adetuyi et al., 2021; Elyasi, 2021; Gazak et al., 2007; Koltai and Fliegel, 2022; Valenzuela and Garrido, 1994).

Natural polyphenolic flavonoids have also prooxidant features in the presence of metal ions due to the formation of phenolic radicals during the exchange of metal ions ($Fe^{3+} \leftrightarrow Fe^{2+}$)(Simunkova et al., 2021; Yordi et al., 2012a). The subsequent interaction of phenolic radicals with oxygen molecules could form reactive oxygen species (ROS) including H_2O_2 (Hodnick et al., 1988; Tian et al., 2021; Zhou and Elias, 2012), which results in cancer cell DNA damage and lipid membrane disruption (Shan et al., 2020; Wang et al., 2019; Zheng et al., 2008). The differential prooxidant impacts observed in cancer cells may be elucidated by the augmented metabolic activity and metallic ion concentrations in the cancerous cells relative to their non-cancerous counterparts. These effects can be effectively exploited in the context of cancer therapy (Chen et al., 2008; Leon-Gonzalez et al., 2015; Simunkova et al., 2021) (Fig. 1A).

Iron is a crucial cellular component that fulfills a significant function in both the conveyance of oxygen and redox reactions. It exists in an elevated concentration within the tumor owing to the excessive expression of transferrin receptors on the malignant cells (Hadi et al., 2007b; Leon-Gonzalez et al., 2015). Iron in the ferrous form has the capability to generate ROS *via* the renowned Fenton reaction, consequently resulting in oxidative stress (Valenzuela and Garrido, 1994) (Fig. 1B). As mentioned above, the polyphenolic compounds' prooxidative property depends on the presence of metal ions. In the current study, we sought to determine whether the increased iron concentrations within the tumor cells could enhance the antitumor effects of silymarin nanoliposomes *via* its prooxidative activity. Therefore, we explored the effect of the concomitant administration of iron sucrose (iron (III)-hydroxide sucrose complex) and silymarin nanoliposomes on the tumor growth and survival of mice bearing tumors.
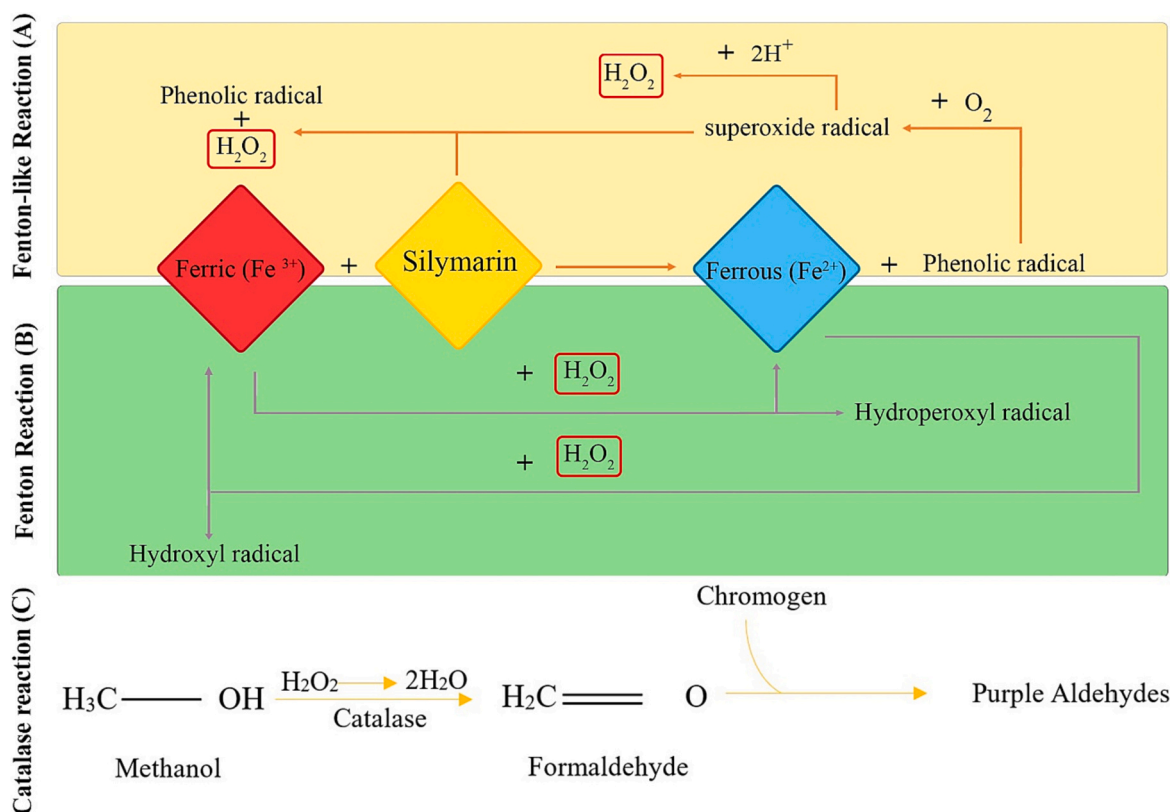

Fig. 1. A. Prooxidant activity of silymarin *via* a phenolic ring in the presence of Fe. The phenolic compounds can reduce iron (Fe^{3+}) resulting in Fe^{2+} and phenolic radicals generation. Phenolic radicals could react with intracellular elements resulting in the production of reactive oxygen species (ROS) with sufficient potential to harm the cell's components including DNA. B. Fenton reaction consumes H_2O_2 and promotes the prooxidant activity in the cells. During the Fenton reaction, iron formations can exchange to each other ($Fe^{3+} \leftrightarrow Fe^{2+}$) in the presence of H_2O_2, and then they increase reactive oxygen species (ROS) which can cause a harmful effect in the host cell. C. Catalase test reaction. Methanol is converted to formaldehyde by catalase enzyme. Catalase mediates the breakdown of hydrogen peroxide into water. Generation of aldehyde chromogen compounds in the presence of formaldehyde can be detected.

2. Materials and methods

2.1. Materials

Silymarin was obtained from Sigma (USA). Roswell Park Memorial Institute 1640 medium (RPMI 1640) was purchased from GIBCO (USA). MTT (3-(4,5-dimethylthiazol-2-yl)-2,5-diphenyltetrazolium bromide) was from Promega (Madison, WI). Hydrogenated soy phosphatidylcholine (HSPC), cholesterol (Chol), and methoxy-polyethylene glycol (MW 2000)–distearoylphosphatidylcholine (mPEG2000–DSPE) and all other phospholipids were purchased from Avanti Polar Lipids (Alabaster, AL). The dialysis bags (12–14 KD) were obtained from Spectrum Laboratories Inc., 4 T1 cell line and female BALB/c mice (aged 8 weeks, 18–20 g) were purchased from Pasteur Institute (Tehran, Iran). Chloroform, methanol, isopropanol, trypan blue was purchased from Merck (Darmstadt, Germany). Intravenous iron sucrose (Venofer) was purchased from Razavi hospital, Mashhad, Iran (ATC code: B03AB02 (WHO)). All other solvents and reagents were used as a chemical grade.

2.2. Liposome Preparation, drug loading, and characterization

Liposomes were prepared according to the previously developed method (Gheybi et al., 2021). Briefly, first SLM-SPC (Silymarin-Soy phosphatidylcholine) complex was synthesized by an overnight incubation of SLM and SPC in acetone as an aprotic solvent, which was then purified by precipitation. To prepare liposomes using lipid film method, chloroform solutions of HSPC: Chol: mPEG$_{2000}$-DSPE and SLM-SPC complex were mixed at 21: 5.6: 1.4: 1.5 M ratios. Organic solvent was then removed by rotary evaporation (Heidolph, Germany) followed by freeze-drying (VD-800F; Taitech, Japan) to form a lipid film. The lipid film was hydrated with HEPES 10 mM containing 10% sucrose (pH 7), using a vortex at 65 °C. The resulting multilamellar vesicles (MLVs) were converted to 100 nm small unilamellar vesicles (SUVs) and were downsized by extrusion through stacked 200, 100, and 50 nm polycarbonate filters with a mini-extruder apparatus (Avanti Polar, USA). To eliminate the unencapsulated silymarin, liposome was dialyzed against HEPES 10 mM containing 10% sucrose (pH = 7.0) for 6 h. The particle size and zeta potential of the liposomes were determined by using a particle size analyzer (Malvern Instruments, Malvern, United Kingdom). The silymarin concentration was measured by diluting the sample 1/100 in methanol, measuring the absorbance at 288 nm, and comparing the absorbance with a standard curve (prepared from a silymarin stock (10 mg silymarin per mL DMSO) diluted in methanol at different concentrations). The intra- and inter-day variation for silymarin was assessed and there was no significant difference between day-to-day analysis. The validation results were established as three repeats for each concentration (7 concentrations).

2.3. In vitro release of silymarin from liposomal formulation

The leakage stability of liposomal formulations was evaluated in PBS solution (phosphate-buffered saline with sodium azide, pH 7). After soaking the dialysis tube in the beaker, 30% FCS was added to silymarin nanoliposome (2 mL) (3:7 *v*/v) and the mixture was placed in dialysis bags (12–14 KD). Dialysis bag was then placed in PBS (100 mL including 200 mg sodium azide) and incubated under stirring at 100 rpm in a sterile situation at 37 °C. During 168 h, sampling was done at 0, 0.5, 1, 2, 3, 6, 12, 24, 48, 72, 96, 120, 144, 168 h by removing 500 μL of each sample from the released medium, which was immediately replaced with 500 μL of fresh PBS buffer. The concentration of silymarin was evaluated as mentioned above.

2.4. Maintenance of cell lines

4 T1 mouse epithelial mammary gland cancer cells, and NI3T3 fibroblast cells isolated from a mouse NIH/Swiss embryo, were obtained from Pasteur Institute, Tehran, Iran. 4 T1 cell was cultured in RPMI supplemented with 10% FBS, 1% streptomycin, and penicillin antibiotics (Pen-Strep). NIH3T3 cells were cultured in DMEM supplemented with 10% FBS, 1% streptomycin, and penicillin antibiotics (Pen-Strep). These cell lines were maintained at a 5% CO$_2$ atmosphere in a humidified incubator at 37 °C.

2.5. In vitro cytotoxicity assays

In vitro cytotoxicity on 4 T1 cells was performed by utilizing MTT viability assay. Briefly, 4 T1 cells were seeded into 96-well microtiter plates at 2500 cells/well. Each plate included positive and blank wells (Untreated cells and medium without cells, respectively). After an overnight incubation at 37 °C, 5% CO$_2$, the medium was carefully aspirated, avoiding the removal of the cells. Then, a fresh medium (200 μL) containing 100 μL of the formulation at different concentrations (0.023, 0.046, 0.093, 0.18, 0.275, 0.75 and 1.5 mM) was added to the wells. Plates were incubated at 37 °C, 5% CO$_2$ for 48 h. Then, the medium was carefully aspirated and replaced with a 100 μL FCS free cell culture medium containing 10 μL of MTT solution. In the living cells, mitochondrial dehydrogenases can convert soluble yellow MTT dye to an insoluble purple formazan precipitate by cleavage of the tetrazolium ring. The insoluble formazan precipitate was then dissolved by adding 200 μL DMSO (Merck, Germany) and its optical density (OD) was read on a multiwell scanning spectrophotometer plate reader at a wavelength of 570 nm *via* Gene5 software. 4 T1 cell-cultured wells containing 200 μL RPMI cell culture medium were used as a positive control in each plate (Langdon, 2004). To evaluate the effect of silymarin nanoliposome and iron sucrose combination, 4 T1 cells were treated with silymarin nanoliposomes (SLM lip) (0.023, 0.046, 0.093, 0.18, 0.275, 0.75 and 1.5 mM), iron sucrose (Fe) (0.0156, 0.031, 0.0625, 0.125, 0.25, 0.5 and 1 mM), iron sucrose and silymarin nanoliposome combination (Fe + SLM lip) (SLM lip+Fe) (at 8:1 and 16:1 M ratio) on two consecutive days, respectively. It is to note that, in the combination treatment, the first drug (Fe or SLM) was removed after 24 h and the second treatment was added.

Relative cell death was calculated as follows:

$$Relative\ cell\ death = 1 - \frac{A\ sample\_A\ blank}{A\ control\_A\ blank}$$

where A sample and A control were the absorbance of the cells treated with the sample solutions and the culture medium (negative control), respectively. A blank was the absorbance of cell free wells. IC$_{50}$ values were calculated using CalcuSyn software (BIOSOFT, UK).

To evaluate the combination response, combination index (CI) was calculated by using CalcuSyn software Version 2.1 (Biosoft, Cambridge, UK). Further, the liposome cytotoxicity was measured in the normal cells compared to the cancer cells to demonstrated drug safe profile.

2.6. Catalase activity assay

Catalase (CAT) is a ubiquitous antioxidant enzyme in the peroxisome organelle of nearly all aerobic cells, which protects cells against oxidative stress-induced damage by catalyzing the decomposition of H$_2$O$_2$ to water and oxygen (Fig. 1C). Furthermore, CAT demonstrates peroxidic activity in which low molecular weight alcohols can serve as electron donors (Farman and Hadwan, 2021; Iwase et al., 2013). We have used the Razi Catalase activity assay kit to measure CAT activity in the biological fluids (TEB, PAZHOUHAN RAZI). This kit measures CAT activity *via* the reaction of the sample CAT with methanol in the presence of an optimal concentration of H$_2$O$_2$ to produce formaldehyde. The formation of formaldehyde is then calorimetrically determined by using a chromogen that turns aldehydes to purple.

For this, 4 T1 cells were suspended in PBS solution (phosphate-buffered saline with sodium azide, pH 7) at 1×10^6 cells/mL. Cells were

lysed *via* freeze/thaw cycles by placing them 5 times at 37 °C and − 70 °C (10 min), respectively. Then, the cell lysate was transferred to a fresh tube and placed on ice for further measurements. Reagents (R1-R7) were prepared at room temperature according to the test guide sheet (Razi Catalase activity assay kit, TEB PAZHOUHAN RAZI, Iran) before performing the assay. The cell lysate in a 96-well plate (20 μL/well) was incubated with the reagents according to the protocol. After the incubation time, the absorbance was read at 540 nm using a plate reader device (Epoch Microplate Spectrophotometer-US)(Zhang et al., 2017).

2.7. Bradford assay

In this study, we have used the Razi Bradford assay kit (TEB PAZ-HOUHAN RAZI, Iran) to determine the total protein contents in the aqueous medium. This kit takes advantage of the color change of Coomassie dye when bind to proteins in an acidic medium. The resulting blue dye protein formation can be easily quantified calorimetrically (595 nm). For this, 4 T1 cells were cultured in RPMI medium culture (1 million per flask) and treated with iron sucrose and silymarin nanoliposome for 24 h. Cells were also treated with the combination of silymarin nanoliposome and iron sucrose as (SLM Lip-Fe) or (Fe-SLM Lip), with 24 h intervals. After cell lysis with freeze/thaw cycles 5 times at 37 °C and − 70 °C, respectively (10 min), the total protein contents of each sample's protein were evaluated by using the Bradford test. In this way, we have equalized and normalized the catalase enzyme activity by total protein in each sample.

The cell lysate in a 96-well plate (10 μL/well) was incubated with the reagents and standards added to each cell according to the protocol. Finally, the absorbance was read at 595 nm immediately utilizing a plate reader (Epoch Microplate Spectrophotometer-Stat Fax-2100, US)(Kielkopf et al., 2020).

2.8. Ethics statement

The protocol involving animals was approved by the Institutional Ethical Committee and Research Advisory Committee of Mashhad University of Medical Sciences (Education Office dated December 05, 2019; proposal code 1398.680), based on the Specific National Ethical Guidelines for Biomedical Research issued by the Research and Technology Deputy of Ministry of Health and Medicinal Education (MOHME) of Iran in 2005.

2.9. Animals

Female BALB/c mice, aged eight weeks old, were purchased from Pasteur Institute, Tehran, Iran. All animals received human care under the institutional guideline based on the approval of the Institutional Ethical Committee and Research Advisory Committee of Mashhad University of Medical Sciences (MUMS) according to animal welfare guidelines. The mice were kept in an animal house of Mashhad *Avicenna* Research Center at 21 °C in a colony room 12/12-h light/dark cycle with free access to water and animal food and kept at 50% relative humidity with 12-h light/dark cycles.

2.10. Antitumor study

The *in vivo* efficacy of silymarin nanoliposomes in combination with injectable iron sucrose was evaluated in female BALB/c mice. Animals were acclimated to the study environment for 2 weeks before the study initiation. On day 0, female BALB/c mice (aged 8 weeks, 18–20 g) were given a subcutaneous injection of 2.5×10^5 4 T1 cells/mouse in the right hind flank, and the tumors were allowed to grow. One week after implantation, animals with palpable tumors were randomized into 5 different treatment groups ($N = 6$) as follows. Mice received a single i.v dose of either iron sucrose (10 mg /kg) (Fe), or SLM Lip (10 mg /kg), silymarin nanoliposome (10 mg /kg) and iron sucrose (10 mg /kg)

combination as iv injections on two consecutive days (SLM Lip + Fe and Fe + SLM Lip, respectively), as well as dextrose 5% as control. In combination treatment, the second drug was administrated 24 h after the first drug. All injections were through the lateral tail vein (Fig. 2). Starting on the day of the treatment, the animals' weight, tumor volume, and overall health were recorded and monitored on 3 occasions a week for 60 days. Three dimensions of the tumor were measured with calipers and the tumor volume was calculated *via* the following formula:

$$\text{Tumor volume} = (\text{height} \times \text{length} \times \text{width}) \times 0.52 \text{ cm}^3$$

For ethical considerations, mice were sacrificed due to a decrease in body weight (>15% loss), tumor enlargement (>2 cm in one dimension), or declining health.

2.11. Histological study

At the end-point of the survival experiment, adult female BALB/c mice (aged 8 weeks and weighing 18–20 g) were anesthetized under an ethical condition. The tissues including liver, kidney, heart, and tumor were collected, scrubbed, and fixed in 10% neutral buffered-formalin. The tissues were then labeled and kept at 4 °C. For analyzing the grafts, samples were washed with 70% alcohol for complete formalin elimination. The serial sections of 7 μm tissues were made with the help of Microtome (Leica Biosystems, Germany). Hematoxylin and eosin-stained slides were prepared using a standard protocol (Jorgensen et al., 2017). The slides were examined under the light microscope 40× (Olympus Company, China) for histological changes. Finally, the necrosis percentage was determined by a histologist(Li et al., 2018).

2.12. Statistical analysis

One-way ANOVA statistical software was used to analyze the data. In the case of significant F value, Tukey–Kramer multiple comparison tests were carried out as a post-test to compare the means in different groups of mice. *$P < 0.05$, **$P < 0.01$, and ***$P < 0.001$ were considered statistically significant.

3. Results

3.1. Characterization of liposomes

The particle size, PDI, and surface charges of the formulation were measured by the Dynamic Light Scattering (DLS) instrument (Nano-ZS; Malvern, UK) as described elsewhere (Riahi et al., 2018). The amounts of phospholipids were determined based on the Bartlett phosphate assay method (Bartlett, 1959). The final liposome's size by number, PDI, and zeta potential were 77.97 ± 3.51 nm, 0.23 ± 0.01, and − 16.5 mV, respectively. SLM concentration in liposomes was 3.31 mM (1.6 mg/ mL).

3.2. In vitro release of silymarin from liposomes

The *in vitro* release of silymarin from liposomal formulations was assessed in 100 mL phosphate-buffered saline with sodium azide at 37 °C. During the first 24 h of incubation at 37 °C, almost 15% drug release was observed from liposomes. By increasing the time to 168 h, the release rate occurred in an approximately monotonous trend (Fig. 3).

3.3. Cytotoxicity of drug combination

The cytotoxicity of silymarin nanoliposome, iron, sucrose, and their combination was assessed using 4 T1 mouse breast cancer cells. The half-maximal inhibitory concentrations (denoted as IC_{50}) of iron sucrose, the liposomes, and their combination after 48 h incubation time are presented in Table 1. As shown in this table, the cytotoxicity of iron
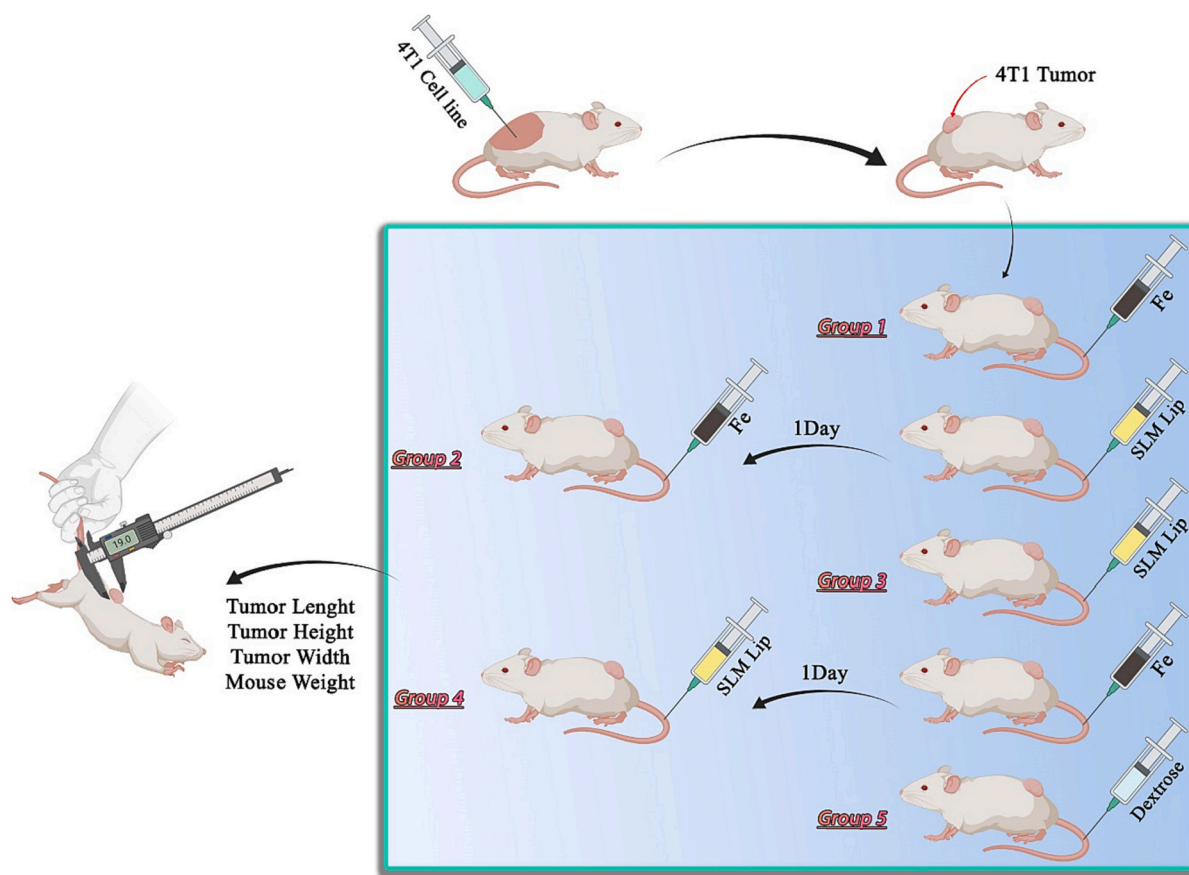
Fig. 2. Project timeline. An animal model study. Mice were distributed in 5 groups randomly and each group received different drugs including control (Dextrose), iron sucrose (Fe), silymarin nanoliposome (SLM Lip), iron sucrose + silymarin nanoliposome (Fe + SLM Lip), and silymarin nanoliposome + iron sucrose (SLM Lip + Fe). Their tumor size, weight, and survival rate have been under surveillance during the period. The results were analyzed using GraphPad Prism version 8.4 software.
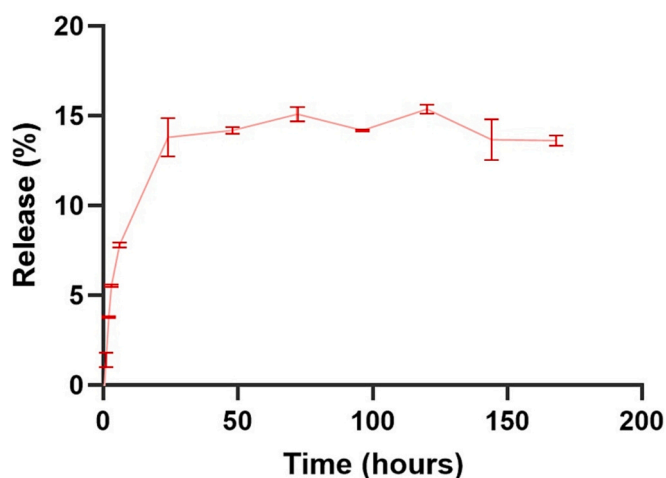

Fig. 3. *In vitro* nanoliposomes (SLM Lip) test. Silymarin nanoliposome (SLM Lip) was added to PBS buffer. The sampling was conducted during a 168 h period and each 500 ul sampling was replaced with fresh PBS buffer (including sodium azide). The results were analyzed *via* GraphPad Prism version 8.4.

Table 1

Cytotoxicity effect (IC$_{50}$) of drugs alone and in combination in 4 T1 cell line.

Formulations		48 Hours	
		IC50 (mM)	CI
Injectable iron sucrose		80.35 ± 20	–
Silymarin nanoliposome		0.03 ± 0.01	–
Combination: 8:1 M ratio	Iron sucrose (Fe)	0.015 ± 0.01	0.51 ± 0.07
Fe + SLM Lip	Silymarin nanoliposome (SLM Lip)	0.16 ± 0.02	
Combination: 16:1 M ratio	Iron sucrose (Fe)	0.19 ± 0.01	0.34 ± 0.09
Fe + SLM Lip	Silymarin nanoliposome (SLM Lip)	0.01 ± 0.05	
Free silymarin		0.16 ± 0.03	–

8:1 and 16:1 M ratio, respectively). Our data indicated that treatment with iron sucrose followed by silymarin nanoliposome has lowered IC$_{50}$ value. In addition, liposomal SLM lower toxicity on the normal cell (NIH3T3) compared to the tumor cell (4 T1) is demonstrated in Fig. 4.

3.4. Antioxidant and prooxidant activity of catalase enzyme

The antioxidant and prooxidant effects of silymarin, nanoliposome, iron, sucrose, and their combination were evaluated *via* catalase enzyme activity assessment. For this, 4 T1 cells were counted and divided between 5 cell flasks, and the Bradford test was utilized to measure the total protein contents in each flask. Therefore, the catalase enzyme activity was normalized based on an equal amount of protein per flasks
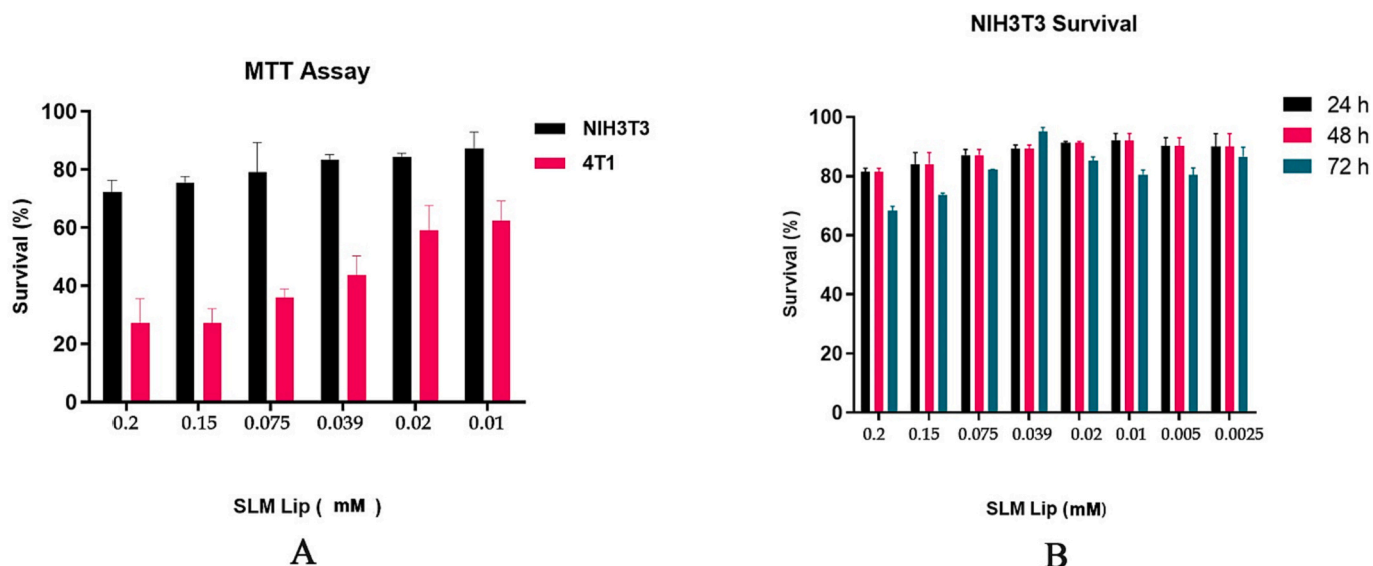
sucrose in combination with silymarin nanoliposomes on the two consecutive days was significantly increased compared to iron sucrose at both 1:8 and 1:16 M ratios. Combination indices <1 indicated a synergistic effect between iron sucrose and silymarin nanoliposomes on the growth inhibition of 4 T1 cells in the 48 h incubation (0.51 and 0.34 at

Fig. 4. Drug safe profile. A. Cell survival rate has been increased in normal cell line (NIH3T3) in compare with tumor cell line (4 T1) with different drug concentration. B. cell survival rate with different drug concentration in three different time period in normal cell line.

(sample). The catalase enzyme activity is shown in Fig. 5 at three different time points. At all-time points, SLM Lip improved the catalase activity compared to control ($p < 0.0001$). Incubation of the cells with free iron sucrose (Fe) did not significantly change the activity of catalase compared to control ($p > 0.0.05$). Data also indicated a significant time-dependent response regarding the combination therapy. In the first 24 h, treatment with the combinations (Fe + SLM Lip and SLM Lip + Fe) resulted in a significantly higher catalase activity compared to the control ($p < 0.001$, $p < 0.0001$ respectively), while by increasing the incubation time to 48 h, the activity of the enzyme showed a significant reduction which was comparable to that of control in both groups ($p < 0.0001$). At 48 h, the catalase enzyme activity following treatment with SLM Lip was significantly higher compared to the combination of iron sucrose and silymarin nanoliposome (Fe + SLM Lip and SLM Lip + Fe) ($p < 0.0001$).

3.5. Anti-tumor effect of liposomes

The antitumor efficacy of silymarin nanoliposome, an injectable iron sucrose, and their combination was evaluated in the 4 T1 tumor-bearing mouse model (total number of animals = 30, 6 mice/group). After tumor induction (Fig. 6A), mice received a single i.v dose of iron sucrose (10 mg /kg), a single i.v dose of silymarin nanoliposome (10 mg /kg), silymarin nanoliposome (10 mg /kg), and iron sucrose iv injections on two consecutive days (10 mg /kg) (SLM Lip+Fe and Fe + SLM Lip), as well as dextrose 5% as control. Mice were monitored for their tumor size, weight, and survival, 3 times a week for 60 days. Tumor volume, mouse weight, and survival are shown in Fig. 6B, C, and D, respectively.

Tumor growth data demonstrated a significant tumor shrinkage ($p < 0.001$) in Fe + SLM Lip combinations when compared to the control group. The SLM Lip treatment as well as its combination with iron
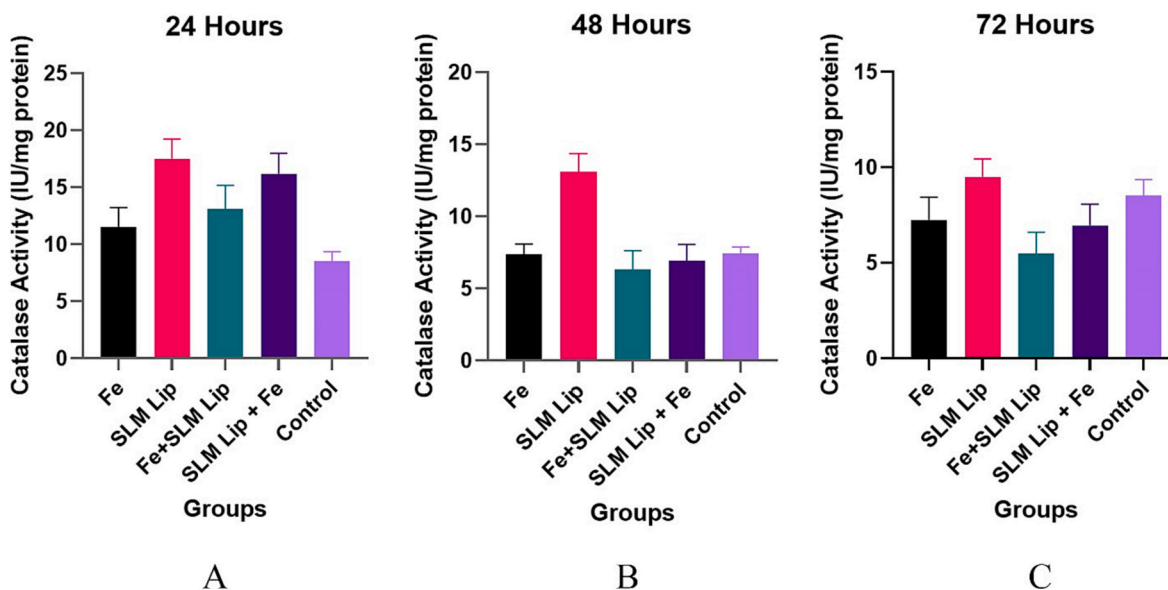

Fig. 5. Catalase enzyme activity. Cells were treated with iron sucrose (Fe), silymarin nanoliposome (SLM Lip), iron sucrose + silymarin nanoliposome (Fe + SLM Lip), silymarin nanoliposome + iron sucrose (SLM Lip + Fe), and control. Then, cell lysis was performed *via* the freeze/thaw method and after centrifuge, the supernatant was added to a 96-well plate. After adding the catalase kit (Razi kit) reagent to the wells, the absorbance of the wells was analyzed with GraphPad Prism version 8.4. A) 24 h B) 48 h C) 72 h.
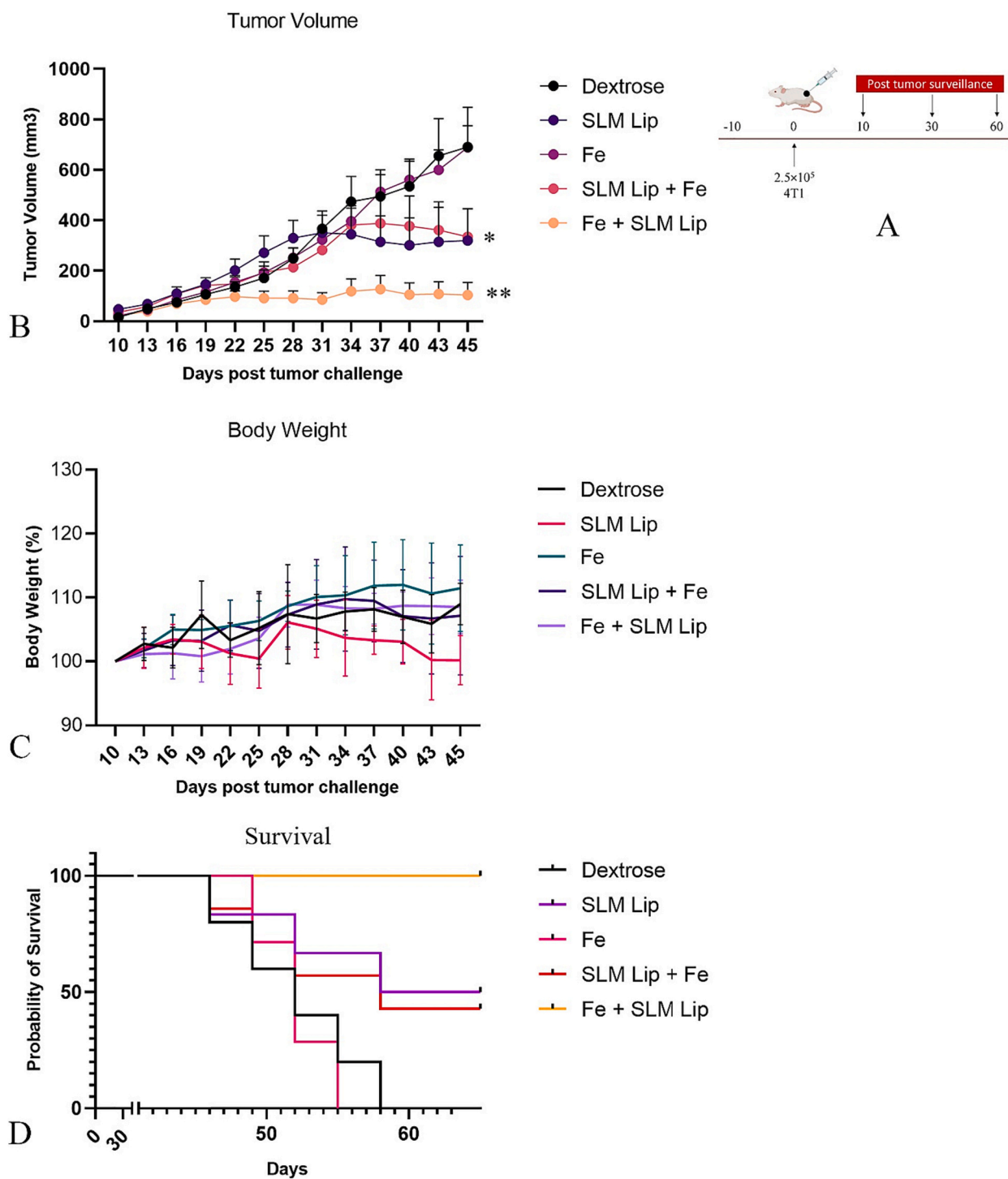
Fig. 6. Therapeutic efficacy of silymarin liposome (SLM Lip), injectable iron sucrose (Fe), and their combination in female breast cancer BALB/c mice models. A. Timeline (days) of tumor inoculation and surveillance of mice. B. The average tumor volume, tumor size of each mouse was measured in 3 dimensions (width, length, and height) by using a digital caliper every second day, and the tumor size of >1000 mm^3 was considered as a dead mouse. C. Bodyweight. D. Survival index of mice. The analysis of therapeutic groups was monitored by the multiple comparison log-rank (Mantel-Cox) test. Effects of treatment on survival time were monitored for a period of 60 days among BALB/c mice ($n = 6$). The Control and iron sucrose (Fe) groups were died out before the 60th day. The iron sucrose + Silymarin nano-liposome group (Fe + SLM Lip) has remained alive until the last day of investigation. All analyses were performed by GraphPad Prism version 8.4.

sucrose (SLM Lip + Fe) showed comparable tumor growth inhibitory effects, which was significantly different compared to control and iron (Fe) groups ($p < 0.01$) (Fig. 6B – Fig. 7). Regarding survival, during 60 days observation, Fe + SLM Lip significantly improved animal survival compared to others ($p < 0.001$). The survival was also significantly improved in the liposomal silymarin and its combination with iron

sucrose (SLM Lip + Fe) compared to the control and iron groups ($p < 0.01$) (Fig. 6D). In general, Fe + SLM Lip showed the maximum survival rate, while other groups indicated an increased mortality rate among animals. The time to reach end point (TTE) for each mouse was calculated from the equation of the line obtained by logarithmic regression of the tumor growth curve. The percent of tumor growth delay (%TGD)
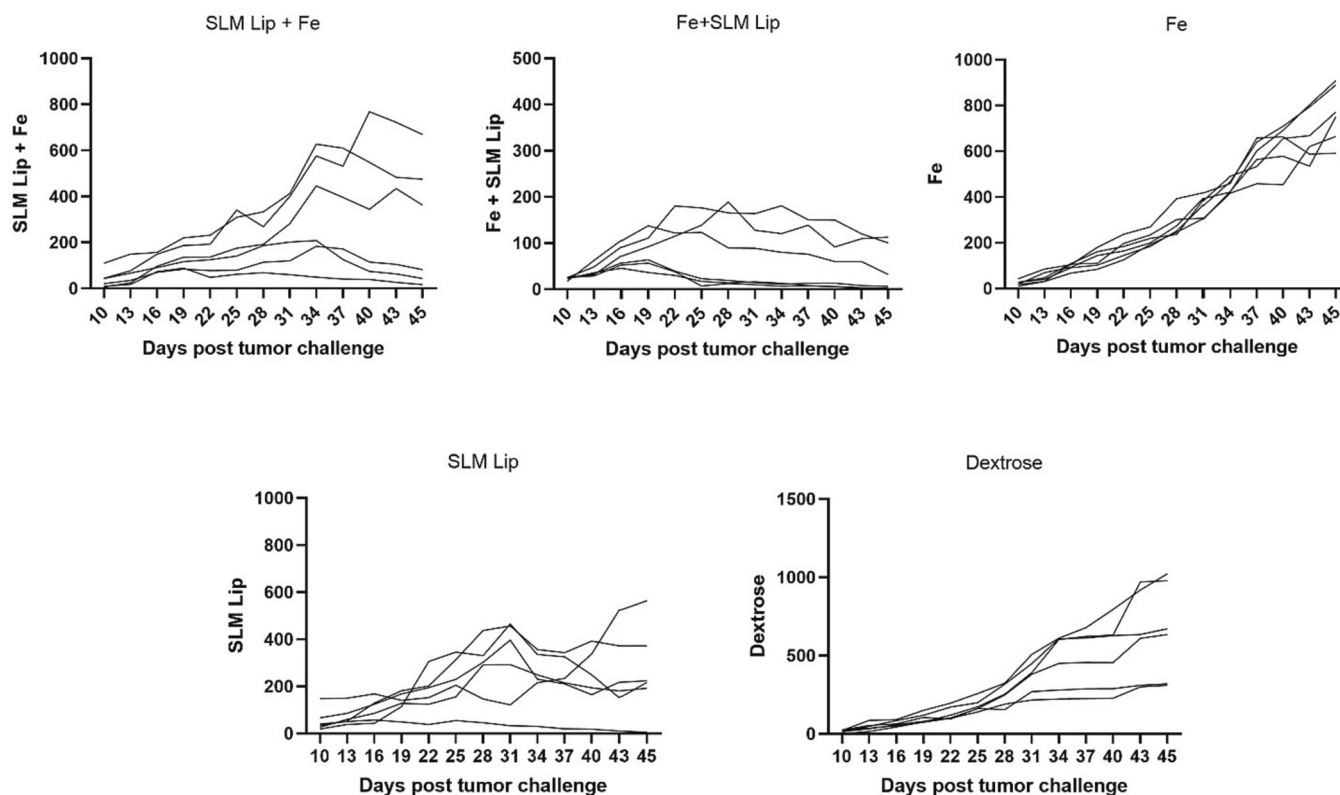
Fig. 7. Comparative tumor volume in different groups of mice during the research days. The tumor size of each mouse in each treatment were compared with the buffer group (n = 6).

was calculated based on the difference between the mean TTE of treatment group (T) and the mean TTE of the control group (C) (Marzban et al., 2015; Schluep et al., 2006).

$$(\%TGD = [(T - C)/C] \times 100)$$

Tumor growth delay (TGD) for each treatment group is also summarized in Table 2. In animals treated with Fe + SLM Lip, it took more time to reach the endpoint and all animals survived until the last day. Moreover, the tumor growth delay in the Fe + SLM Lip group was higher compared to its peers in other groups. The mouse weights did not demonstrate significant differences among all treatment groups (Fig. 6C).

3.6. Histological examination

Hematoxylin-eosin staining was utilized to evaluate the histology of tumors in mice. The histological examination of mouse tissues demonstrated that there was no injury to the liver, heart, and kidneys of any

Table 2
Survival parameters of treated mice.

Formulations	MST[a] (day) (n = 6 per group)	TTE[b] (days ± SD)	TGD[c] (%)
Control (Dextrose)	52	52 ± 4.7	–
Iron sucrose (Fe)	52	61 ± 5.8	17.3
Silymarin nanoliposome (SLM Lip)	55	52 ± 2.4	0
Silymarin nanoliposome + Fe (SLM Lip + Fe)	55	57 ± 8.2	9.8
Fe + Silymarin nanoliposome (Fe + SLM Lip)	Undefined	65 ± 0.0	25

[a] Median survival times.
[b] Time to reach an endpoint.
[c] Tumor Growth Delay %.

mouse in all treatment groups. As illustrated in Fig. 8, significant tumor tissue necrosis was observed in all groups. The greatest tumor necrosis and tumor tissue damage were observed in mice treated with Fe + SLM Lip. The rate of tumor necrosis was 45% in Fe + SLM Lip, 30% in SLM Lip, 20% in Fe and SLM Lip + Fe, and 10% in Dextrose. Furthermore, considerable metastasis invasion in the control group (dextrose) was observed compared to Fe + SLM Lip in the digestive intestine and pancreatic tissues of animals (Fig. 9).

4. Discussion

In recent decades, there has been a significant increase in the incidence and mortality rates of cancer, thereby rendering it as one of the most fatal diseases globally (Ferlay et al., 2021). Chemotherapy resistance and its associated adverse effects continue to pose significant challenges in the pursuit of successful cancer treatment. Consequently, the quest for alternative therapies represents a crucial undertaking in the management of cancer (Amjad et al., 2021). The utilization of herbal medicines has garnered a significant interest due to the efficacy and minimal adverse effects on the human body (Kwon et al., 2021). Silymarin has demonstrated noteworthy antioxidative potential due to its capacity to protect cells from ROS and other free radicals. The antioxidative activity of silymarin is linked to the oxidation of the silybin molecule's 2–3 carbon positions and the production of 2–3 dihydrostilbenoid, which exhibits significantly greater antioxidative efficacy than silybin (Farjad and Momeni, 2018; Koltai and Fliegel, 2022). Despite the surge of investigations into the antioxidant activity of silymarin, animal models studies have not been carried out to illustrate the therapeutic efficacy *in vivo* as much as expected (Caon et al., 2021; Ghareeb, 2021; Lomozova et al., 2021).

Studies also indicate that polyphenolic compounds possess a significant potential to exhibit pro-oxidant activity in specific circumstances, particularly in the presence of metallic ions (Leon-Gonzalez et al., 2015).
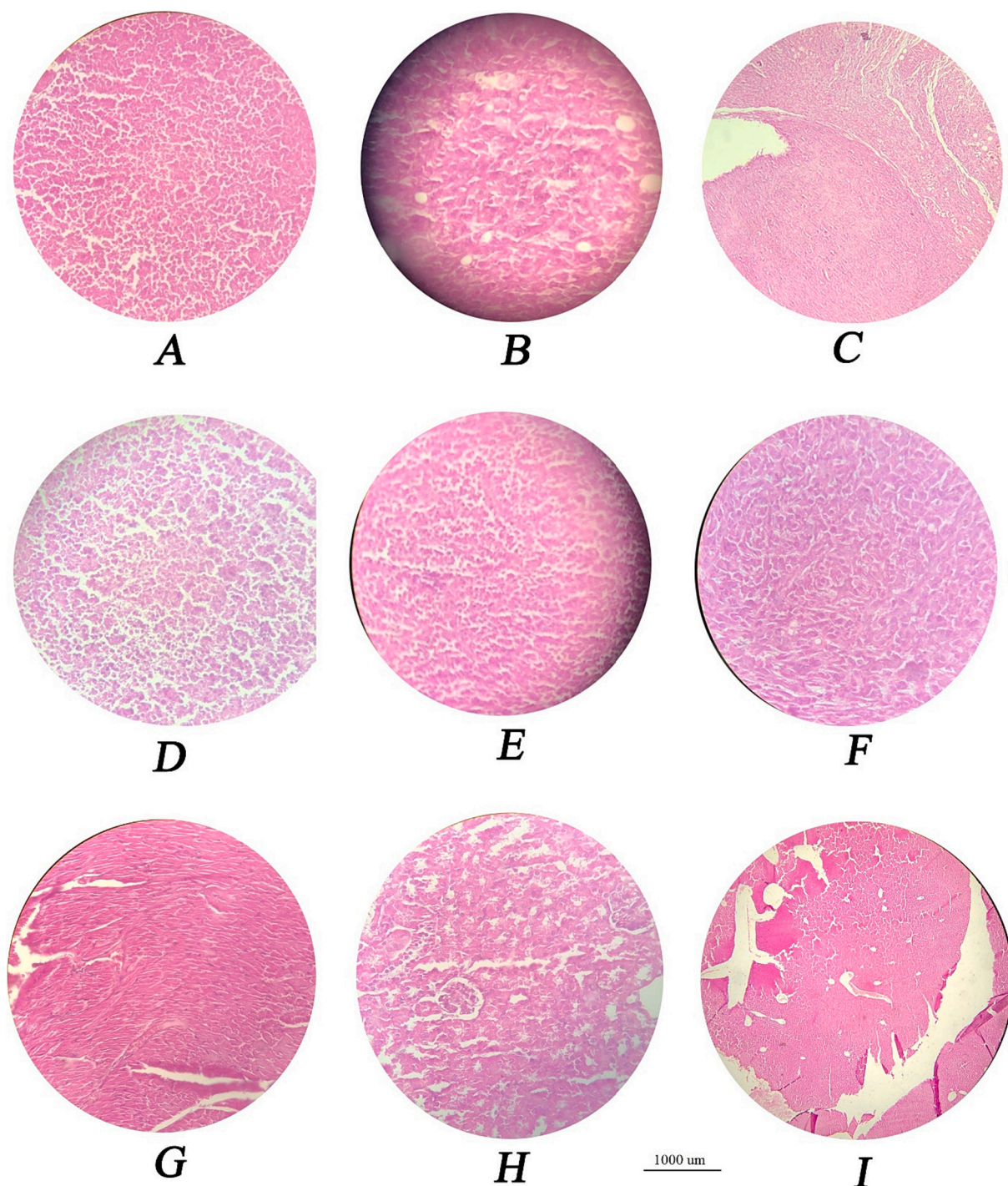
Fig. 8. Tumor tissue of separate mouse groups. Mice were anesthetized under ethical measurements and their tissues (liver, kidney, heart, and tumor) were fixed in formalin buffer 10%. Then, the analysis of tissue necrosis was performed by the hematoxylin-eosin staining method. A&B. Necrosis in iron sucrose + Silymarin nanoliposome group (Fe + SLM Lip) contains 45%. C. Necrosis in the control group (Dextrose) contains 10%. D. The silymarin nanoliposome group (SLM Lip) tumor contains 30% necrosis. E&F. Iron sucrose (Fe) and Silymarin nanoliposome + iron (SLM, Lip + Fe) sucrose groups which contain 20% necrosis in tumor tissue. G. Heart tissue of iron sucrose + Silymarin nanoliposome group (Fe + SLM Lip) which is sound and without pathologic conditions. H. Kidney tissue of iron sucrose + Silymarin nanoliposome group (Fe + SLM Lip) which is sound and without pathologic conditions. I. Liver tissue of iron sucrose + Silymarin nanoliposome group (Fe + SLM Lip) is sound and without pathologic conditions.

Although the potential deleterious effects of polyphenolic combinations' prooxidant activity on the tumor cells have been noted, inadequate research has been undertaken to exploit this potential in experimental and clinical settings. Although previous studies have demonstrated silymarin's chemo-preventive effect due to its antioxidant properties, our research delves deeper into the antioxidant-to-prooxidant transformation aspect (Delmas et al., 2020; El-Awady el et al., 2011; Schroder et al., 2005), and we observed efficient tumor cell death following combination of liposomal silymarin with iron (*in vitro*). In addition, further necrosis in the tumor tissue was observed following treatment with the combination regimen (Fe + SLM Lip) compared to liposomal silymarin alone *in vivo*.
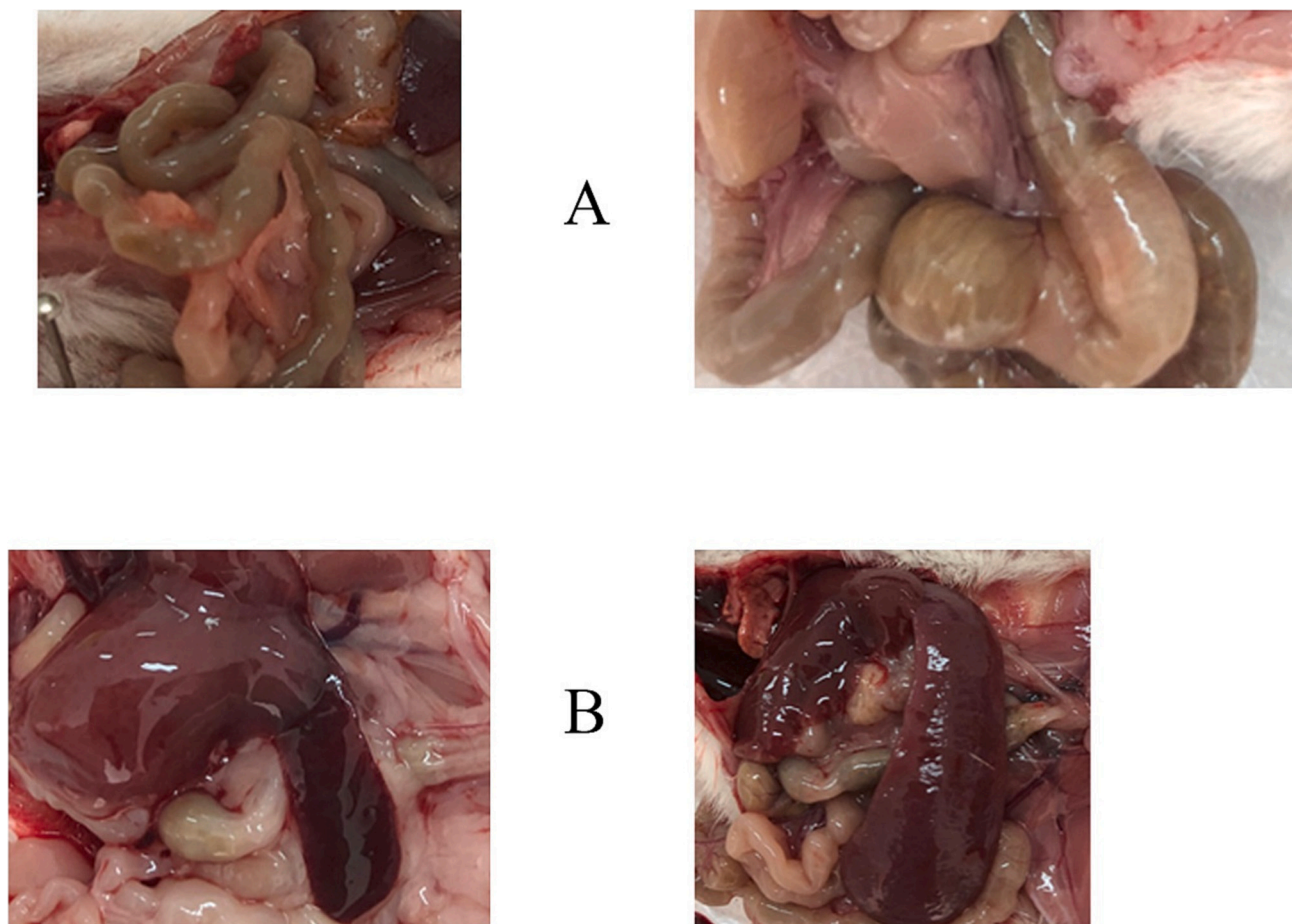
Fig. 9. Comparing tissues' metastasis in the control group (Dextrose) and the group that received iron sucrose + Silymarin nanoliposome (Fe + SLM Lip). A. Metastasis in intestine tissue (left is iron sucrose + Silymarin nanoliposome group (Fe + SLM Lip) and the right belongs to control group (Dextrose)). B. Metastasis in pancreatic tissue (left is iron sucrose + Silymarin nanoliposome group (Fe + SLM Lip) and the right belongs to control group (Dextrose)).

Therapeutic agents, encompassing both naturally occurring and synthetic compounds, which target diverse facets of iron metabolism and ROS homeostasis, have exhibited auspicious outcomes in cancer treatment (Bystrom et al., 2014; Chaston et al., 2004). Cumulative pieces of evidence suggest the major role of ROS in the initiation and promotion of carcinogenesis and resistance to apoptosis. This increased ROS level in the tumor cells, known as "oxidative stress", is partly due to the elevated rate of metabolism and alterations to glycolysis where excessive ROS accumulation overwhelms cellular defenses (Panayiotidis, 2008; Ziech et al., 2011). While the employment of antioxidant agents to reduce levels of ROS has been shown to potentially revert the malignant phenotype of the cancer cells, it must be noted that elevated levels of ROS can lead to oxidative harm of crucial biomolecules such as DNA, proteins, and lipids (Leon-Gonzalez et al., 2015; Valko et al., 2007). Intracellular antioxidant enzymes including catalase have shown alteration in several cancers, which serves as a potential survival benefit for the cancer cells (Kang et al., 2013; Ladelfa et al., 2011).

In the current study, silymarin nanoliposomes showed higher toxicity on 4 T1 cells when combined with iron sucrose. We also observed that exposing the cells to iron sucrose and the consecutive treatment with SLM Lip (Fe + SLM Lip) induced greater toxicity compared to SLM Lip + Fe. It seems that the accumulation of iron ions (Fe^{3+}) is a prerequisite for triggering the prooxidant activity of SLM Lip. Furthermore, combination therapy with Fe + SLM Lip showed a time-dependent effect on lowering the catalase activity compared to SLM Lip alone. Our observation indicated that while iron sucrose did not alter cell toxicity and catalase activity, the antioxidant feature of SLM Lip was

clearly demonstrated by increasing the catalase activity *in vitro*. Iron entry into the cancer cells could likely alter the antioxidant trait of SLM. As previously mentioned, polyphenolic compounds in reaction with ferric ions generate ferrous ions and phenolic radicals. Consequently, ROS species including O_2^- are produced following the reaction of phenolic radicals and intracellular O2, and the resulting radicals can subsequently generate H_2O_2 when reacting with the hydrogen ions (Eghbaliferiz and Iranshahi, 2016). In this way, increased free radicals (ROS) can induce cellular death by damaging the vital macromolecules within the cells (Leon-Gonzalez et al., 2015; Salnikow, 2021; Simunkova et al., 2021; Zhou and Elias, 2012). In addition, the generated Fe^{2+} can react with H_2O_2 and trigger the Fenton reaction (Shen et al., 2019; Yan et al., 2020). By exchanging iron species during the Fenton reaction ($Fe^{3+} \leftrightarrow Fe^{2+}$), the ROS levels could increase (Simunkova et al., 2021). Therefore, in the Fenton reaction, H_2O_2 free radicals are consumed (Fig. 1B) (Pérez-Gonzalez et al., 2022). Thus, the reduced catalase activity following Fe + SLM Lip treatment might clarify the role of the Fenton reaction, during which intracellular H_2O_2 is utilized, which could be regarded as an indicator of the prooxidant activity of the iron-SLM combination.

Previously, the prooxidant activity of polyphenol compounds and the role of the transition metals have been explicated. Studies have demonstrated that the reduction of metal ions can play a part in redox cycling, which amplifies the production of free radicals *via* the Fenton reaction, culminating in the fragmentation of cellular DNA (Hadi et al., 2007a). Therefore, iron accumulation in the tumor cells could induce the prooxidant activity of the polyphenolic compounds and ROS generation inside the target cell (Leon-Gonzalez et al., 2015; Yan et al.,

2018; Yordi et al., 2012b), causing tumor cell annihilation (Jomová et al., 2019). Further, increasing ROS levels have shown to induce ferroptotic cell death and iron-mediated ROS production by Fenton reaction (Dixon et al., 2012; Xie et al., 2016). The Fenton reaction can damage the cell's components like DNA, so this mechanism is widely utilized for cancer therapy (Imlay et al., 1988; Qian et al., 2019). Of note, ferroptosis-triggering nanoparticles have also been explored in cancer therapy investigations (Lin et al., 2018; Liu et al., 2019; Shen et al., 2018). Recently, numerous nanotherapeutics have been administrated to initiate the Fenton reaction in the cancer cells (Huo et al., 2019; Qian et al., 2019). For instance, Li et al. tried to indirectly deliver H_2O_2 and ferric ions into the cancer cells *via* a nanocatalyst carrier to trigger the Fenton reaction (Li et al., 2016). In this way, the SLM nanoliposome used in this study might be regarded as a nanocatalyst that can initiate the generation of ROS in the target tumor, when administered with iron ions which could potentially eliminate the tumor cells.

The *in vivo* bioavailability of silymarin flavonolignans is poor due to low aqueous solubility. However, the *in vivo* effectiveness of silymarin could be ameliorated when encapsulated into liposome (Fahr et al., 2005; van Hoogevest et al., 2011). SLM Lip used in the current study could successfully reach the target tumor tissue based on the well-known EPR phenomenon (Enhanced Permeation and Retention Effects) (Maeda, 2021). It has been demonstrated that liposomes with approximately 100 nm in size could accumulate in the tumor site through the EPR effect (Maeda, 2021). Furthermore, the homogeneous population of liposomal formulations as well as the negative surface charge contributed to their *in vivo* stability within the circulation (Chen et al., 2015). When tested in animal models, the therapeutic efficacy of SLM Lip along with iron sucrose (Fe + SLM Lip) was superior compared to SLM Lip in breast tumor-bearing mice. Our observations indicated that Fe + SLM Lip-treated animals survived during the study period. To our knowledge, this is the first time that the prooxidant activity of SLM liposomes is investigated in an animal model with breast cancer. The histopathological studies demonstrated no injury to the major organs in animals in any of the treatment groups, while partial tumor necrosis was observed with the greatest ratio in (Fe + SLM Lip) and lowest in iron sucrose, (SLM Lip + Fe) and dextrose (45, 20 and 10%, respectively) groups. Furthermore, a remarkable metastasis invasion in the digestive tissues of animals was observed in controls compared to Fe + SLM Lip.

The present study exhibited that the build-up of iron within the neoplastic cells located in the tumor tissue has the potential to elicit a pro-oxidative trait of SLM Lip that has accumulated at the tumor site. Consequently, the ensuing generation of free radicals, predominantly ROS, may result in harmful alterations to intracellular components and eventual cellular demise (Harris and DeNicola, 2020; NavaneethaKrishnan et al., 2019). The accumulation of both iron (Fe) and SLM-Lip moieties in the tumor area plays a significant role in inducing selective cytotoxic effects in cancer cells (Simunkova et al., 2021; Yordi et al., 2012b).

5. Conclusion

In the present investigation, the effects of SLM Lip in conjunction with iron sucrose (Fe) was examined against breast cancer *in vitro* and *in vivo*. The aforementioned combination exhibited encouraging cytotoxicity, culminating in extended survival and tumor reduction in mice harboring 4 T1 breast tumors, without affecting healthy tissues. As a whole, the results of the contemporary study undeniably showcase the therapeutic potential of merging SLM Lip, and iron for cancer treatment.

Author contribution

Conception and design: Fatemeh Gheybi.
Material preparation, data collection: Maham Doagooyan, Kebria Houshangi, Zahra Khoddamipour.
Analysis: Seyedeh Hoda Alavizadeh, Amirhossein Sahebkar.
Writing-original draft: Maham Doagooyan and Fatemeh Gheybi.
Writing-review and editing: Seyedeh Hoda Alavizadeh, Amirhossein Sahebkar.

Declaration of Competing Interest

The authors declare the following financial interests/personal relationships which may be considered as potential competing interests:
Maham Doagooyan reports financial support was provided by Medical Biotechnology and Nanotechnology Department, Mashhad University of Medical Sciences (MUMS).

Data availability

The datasets analyzed during the current study are available from the corresponding author on reasonable request.

References

Abenavoli, L., Capasso, R., Milic, N., Capasso, F., 2010. Milk thistle in liver diseases: past, present, future. Phytother. Res. 24, 1423–1432.

Adetuyi, F.K., Omolabi, F.K., Olajide, P.A., Oloke, J.K., 2021. Pharmacological, biochemical and therapeutic potential of milk Thistle (Silymarin): a review. World News Nat. Sci. 37, 75–91.

Amjad, M.T., Chidharla, A., Kasi, A., 2021. Cancer Chemotherapy. StatPearls [Internet].

Bartlett, G.R., 1959. Phosphorus assay in column chromatography. J. Biol. Chem. 234, 466–468.

Basak, S., Singh, J.K., Morri, S., Shetty, P.H., 2021. Assessment and modelling the antibacterial efficacy of vapours of cassia and clove essential oils against pathogens causing foodborne illness. LWT 150, 112076.

Bernstein, I.L., Webster, M.M., 2021. Learned food aversions: a consequence of cancer chemotherapy, cancer, nutrition, and eating behavior. Routledge 103–116.

Bonifacio, B.V., Silva, P.B., Ramos, M.A., Negri, K.M., Bauab, T.M., Chorilli, M., 2014. Nanotechnology-based drug delivery systems and herbal medicines: a review. Int. J. Nanomedicine 9, 1–15.

Borri, F., Granaglia, A., 2021. Pathology of triple negative breast cancer. In: Seminars in Cancer Biology. Elsevier, pp. 136–145.

Bystrom, L.M., Guzman, M.L., Rivella, S., 2014. Iron and reactive oxygen species: friends or foes of cancer cells? Antioxid. Redox Signal. 20, 1917–1924.

Caon, G., Morrone, M., Feistauer, L., Sganzerla, D., Moreira, J.C., 2021. Moderate beer consumption promotes silymarin-like redox status without affecting the liver integrity in vivo. Food Biosci. 43, 101307.

Chaston, T.B., Watts, R.N., Yuan, J., Richardson, D.R., 2004. Potent antitumor activity of novel iron chelators derived from di-2-pyridylketone isonicotinoyl hydrazone involves Fenton-derived free radical generation. Clin. Cancer Res. 10, 7365–7374.

Chen, Q., Espey, M.G., Sun, A.Y., Pooput, C., Kirk, K.L., Krishna, M.C., Khosh, D.B., Drisko, J., Levine, M., 2008. Pharmacologic doses of ascorbate act as a prooxidant and decrease growth of aggressive tumor xenografts in mice. Proc. Natl. Acad. Sci. U. S. A. 105, 11105–11109.

Chen, X., Zou, L.Q., Niu, J., Liu, W., Peng, S.F., Liu, C.M., 2015. The stability, sustained release and cellular antioxidant activity of curcumin nanoliposomes. Molecules 20, 14293–14311.

Chen, T., Liu, W., Xiong, S., Li, D., Fang, S., Wu, Z., Wang, Q., Chen, X., 2019. Nanoparticles mediating the sustained Puerarin Release facilitate improved brain delivery to treat Parkinson's Disease. ACS Appl. Mater. Interfaces 11, 45276–45289.

Deep, G., Singh, R.P., Agarwal, C., Kroll, D.J., Agarwal, R., 2006. Silymarin and silibinin cause G1 and G2-M cell cycle arrest via distinct circuitries in human prostate cancer PC3 cells: a comparison of flavanone silibinin with flavanolignan mixture silymarin. Oncogene 25, 1053–1069.

Delmas, D., Xiao, J., Vejux, A., Aires, V., 2020. Silymarin and cancer: a dual strategy in both in Chemoprevention and Chemosensitivity. Molecules 25, 2009.

Dixon, S.J., Lemberg, K.M., Lamprecht, M.R., Skouta, R., Zaitsev, E.M., Gleason, C.E., Patel, D.N., Bauer, A.J., Cantley, A.M., Yang, W.S., Morrison 3rd, B., Stockwell, B.R.,

2012. Ferroptosis: an iron-dependent form of nonapoptotic cell death. Cell 149, 1060–1072.

Dorling, L., Carvalho, S., Allen, J., Parsons, M.T., Fortuno, C., González-Neira, A., Heijl, S.M., Adank, M.A., Ahearn, T.U., Andrulis, I.L., 2022. Breast cancer risks associated with missense variants in breast cancer susceptibility genes. Genome Medicine 14, 51.

Eghbaliferiz, S., Iranshahi, M., 2016. Prooxidant activity of polyphenols, flavonoids, anthocyanins and carotenoids: updated review of mechanisms and catalyzing metals. Phytother. Res. 30, 1379–1391.

El-Awady el, S.E., Moustafa, Y.M., Abo-Elmatty, D.M., Radwan, A., 2011. Cisplatin-induced cardiotoxicity: mechanisms and cardioprotective strategies. Eur. J. Pharmacol. 650, 335–341.

Elyasi, S., 2021. *Silybum marianum*, Antioxidant Activity, and Cancer Patients, Cancer. Elsevier, pp. 483–493.

Ezzati, M., Yousefi, B., Velaei, K., Safa, A., 2020. A review on anti-cancer properties of Quercetin in breast cancer. Life Sci. 248, 117463.

Fahr, A., van Hoogevest, P., May, S., Bergstrand, N., Leigh, M.L., 2005. Transfer of lipophilic drugs between liposomal membranes and biological interfaces: consequences for drug delivery. Eur. J. Pharm. Sci. 26, 251–265.

Farjad, E., Momeni, H., 2018. Silymarin ameliorates oxidative stress and enhances antioxidant defense system capacity in cadmium-treated mice. Cell J. 20 (3), 422–426. https://doi.org/10.22074/cellj.2018.5355. Introduction Cadmium is a heavy metal and an environmental pollutant.

Farman, A.A., Hadwan, M.H., 2021. Simple kinetic method for assessing catalase activity in biological samples. MethodsX 8, 101434.

Ferlay, J., Soerjomataram, I., Dikshit, R., Eser, S., Mathers, C., Rebelo, M., Parkin, D.M., Forman, D., Bray, F., 2015. Cancer incidence and mortality worldwide: sources, methods and major patterns in GLOBOCAN 2012. Int. J. Cancer 136, E359–E386.

Ferlay, J., Colombet, M., Soerjomataram, I., Parkin, D.M., Pineros, M., Znaor, A., Bray, F., 2021. Cancer statistics for the year 2020: an overview. Int. J. Cancer 149, 778–789.

Gazak, R., Walterova, D., Kren, V., 2007. Silybin and silymarin–new and emerging applications in medicine. Curr. Med. Chem. 14, 315–338.

Ghareeb, O.A., 2021. Toxicopathological effects of zinc oxide nanoparticles on the liver function and preventive role of silymarin in vivo. Indian J. Forens. Med. Toxicol. 15, 3213.

Gheybi, F., Alavizadeh, S.H., Rezayat, S.M., Hatamipour, M., Akhtari, J., Faridi Majidi, R., Badiee, A., Jaafari, M.R., 2021. pH-sensitive PEGylated liposomal silybin: synthesis, in vitro and in vivo anti-tumor evaluation. J. Pharm. Sci. 110, 3919–3928.

Hadi, S., Bhat, S.H., Azmi, A.S., Hanif, S., Shamim, U., Ullah, M., 2007a. Oxidative breakage of cellular DNA by plant polyphenols: a putative mechanism for anticancer properties. In: Seminars in Cancer Biology. Elsevier, pp. 370–376.

Hadi, S.M., Bhat, S.H., Azmi, A.S., Hanif, S., Shamim, U., Ullah, M.F., 2007b. Oxidative breakage of cellular DNA by plant polyphenols: a putative mechanism for anticancer properties. Semin. Cancer Biol. 17, 370–376.

Harris, I.S., DeNicola, G.M., 2020. The complex interplay between antioxidants and ROS in cancer. Trends Cell Biol. 30, 440–451.

Hashemi Goradel, N., Ghiyami-Hour, F., Jahangiri, S., Negahdari, B., Sahebkar, A., Masoudifar, A., Mirzaei, H., 2018. Nanoparticles as new tools for inhibition of cancer angiogenesis. J. Cell. Physiol. 233, 2902–2910.

Hodnick, W.F., Kalyanaraman, B., Pritsos, C.A., Pardini, R.S., 1988. The production of hydroxyl and semiquinone free radicals during the autoxidation of redox active flavonoids. Basic Life Sci. 49, 149–152.

Huo, M., Wang, L., Wang, Y., Chen, Y., Shi, J., 2019. Nanocatalytic tumor therapy by single-atom catalysts. ACS Nano 13, 2643–2653.

Imlay, J.A., Chin, S.M., Linn, S., 1988. Toxic DNA damage by hydrogen peroxide through the Fenton reaction in vivo and in vitro. Science 240, 640–642.

Iwase, T., Tajima, A., Sugimoto, S., Okuda, K., Hironaka, I., Kamata, Y., Takada, K., Mizunoe, Y., 2013. A simple assay for measuring catalase activity: a visual approach. Sci. Rep. 3, 3081.

Jomová, K., Hudecova, L., Lauro, P., Simunkova, M., Alwasel, S.H., Alhazza, I.M., Valko, M., 2019. A switch between antioxidant and prooxidant properties of the phenolic compounds myricetin, morin, 3′, 4′-dihydroxyflavone, taxifolin and 4-hydroxy-coumarin in the presence of copper (II) ions: a spectroscopic, absorption titration and DNA damage study. Molecules 24, 4335.

Jorgensen, A.S., Rasmussen, A.M., Andersen, N.K.M., Andersen, S.K., Emborg, J., Roge, R., Ostergaard, L.R., 2017. Using cell nuclei features to detect colon cancer tissue in hematoxylin and eosin stained slides. Cytometry A 91, 785–793.

Kang, M.Y., Kim, H.B., Piao, C., Lee, K.H., Hyun, J.W., Chang, I.Y., You, H.J., 2013. The critical role of catalase in prooxidant and antioxidant function of p53. Cell Death Differ. 20, 117–129.

Kielkopf, C.L., Bauer, W., Urbatsch, I.L., 2020. Bradford assay for determining protein concentration. Cold Spring Harb Protoc 2020, 102269.

Koltai, T., Fliegel, L., 2022. Role of silymarin in cancer treatment: facts, hypotheses, and questions. J. Evid. Based Integr. Med. 27, 2515690X211068826.

Krohne, H.W., 2017. Stress Und Stressbewältigung Bei Operationen. Springer.

Kwon, C.Y., Lee, B., Kong, M., Lee, S.H., Jung, H.J., Kim, K.I., Lee, B.J., 2021. Effectiveness and safety of herbal medicine for cancer-related fatigue in lung cancer survivors: a systematic review and meta-analysis. Phytother. Res. 35, 751–770.

Ladelfa, M.F., Toledo, M.F., Laiseca, J.E., Monte, M., 2011. Interaction of p53 with tumor suppressive and oncogenic signaling pathways to control cellular reactive oxygen species production. Antioxid. Redox Signal. 15, 1749–1761.

Langdon, S.P., 2004. Cancer Cell Culture: Methods and Protocols. Springer Science & Business Media.

Leon-Gonzalez, A.J., Auger, C., Schini-Kerth, V.B., 2015. Pro-oxidant activity of polyphenols and its implication on cancer chemoprevention and chemotherapy. Biochem. Pharmacol. 98, 371–380.

Li, H., Dong, L., Liu, Y., Wang, G., Wang, G., Qiao, Y., 2014. Biopharmaceutics classification of puerarin and comparison of perfusion approaches in rats. Int. J. Pharm. 466, 133–138.

Li, W.P., Su, C.H., Chang, Y.C., Lin, Y.J., Yeh, C.S., 2016. Ultrasound-induced reactive oxygen species mediated therapy and imaging using a fenton reaction activable polymersome. ACS Nano 10, 2017–2027.

Li, Y., Li, N., Yu, X., Huang, K., Zheng, T., Cheng, X., Zeng, S., Liu, X., 2018. Hematoxylin and eosin staining of intact tissues via delipidation and ultrasound. Sci. Rep. 8, 12259.

Lin, H., Chen, Y., Shi, J., 2018. Nanoparticle-triggered in situ catalytic chemical reactions for tumour-specific therapy. Chem. Soc. Rev. 47, 1938–1958.

Liu, M., Liu, B., Liu, Q., Du, K., Wang, Z., He, N., 2019. Nanomaterial-induced ferroptosis for cancer specific therapy. Coord. Chem. Rev. 382, 160–180.

Lomozova, Z., Tvrdy, V., Hrubsa, M., Catapano, M.C., Macakova, K., Biedermann, D., Kucera, R., Kren, V., Mladenka, P., Valentova, K., 2021. Dehydroflavonolignans from silymarin potentiate transition metal toxicity in vitro but are protective for isolated erythrocytes ex vivo. Antioxidants (Basel) 10, 679.

Maeda, H., 2021. The 35th anniversary of the discovery of EPR effect: a new wave of nanomedicines for tumor-targeted drug delivery-personal remarks and future prospects. J. Pers. Med. 11, 229.

Marzban, E., et al., 2015. Optimizing the therapeutic efficacy of cisplatin PEGylated liposomes via incorporation of different DPPG ratios: In vitro and in vivo studies. Colloids and Surfaces B: Biointerfaces 136, 885–891.

NavaneethaKrishnan, S., Rosales, J.L., Lee, K.-Y., 2019. ROS-mediated cancer cell killing through dietary phytochemicals. In: Oxidative Medicine and Cellular Longevity 2019.

Panayiotidis, M., 2008. Reactive oxygen species (ROS) in multistage carcinogenesis. Cancer Lett. 266, 3–5.

Pérez-Gonzalez, G., Melin, V., Mendez-Rivas, C., Díaz, J., Moreno, N., Contreras, D., 2022. Role of perhydroxyl radical in the chelator-mediated Fenton reaction. New J. Chem 46, 4884–4889.

Qian, X., Zhang, J., Gu, Z., Chen, Y., 2019. Nanocatalysts-augmented Fenton chemical reaction for nanocatalytic tumor therapy. Biomaterials 211, 1–13.

Ramasamy, K., Agarwal, R., 2008. Multitargeted therapy of cancer by silymarin. Cancer Lett. 269, 352–362.

Redd, W.H., Burish, T.G., Andrykowski, M.A., 2021. Aversive Conditioning and Cancer Chemotherapy, Cancer, Nutrition, and Eating Behavior. Routledge, pp. 117–132.

Riahi, M.M., Sahebkar, A., Sadri, K., Nikoofal-Sahlabadi, S., Jaafari, M., 2018. Stable and sustained release liposomal formulations of celecoxib: in vitro and in vivo anti-tumor evaluation. Int. J. Pharm. 540, 89–97.

Salnikow, K., 2021. Role of Iron in Cancer, Seminars in Cancer Biology. Elsevier, pp. 189–194.

Sanati, M., Afshari, A.R., Aminyavari, S., Kesharwani, P., Jamialahmadi, T., Sahebkar, A., 2023. RGD-engineered nanoparticles as an innovative drug delivery system in cancer therapy. J. Drug Deliv. Sci. Technol. 84.

Schluep, T., et al., 2006. Preclinical efficacy of the camptothecin-polymer conjugate IT-101 in multiple cancer models. Clin Cancer Res 12 (5), 1606–1614.

Schroder, F.H., Roobol, M.J., Boeve, E.R., de Mutsert, R., Zuijdgeest-van Leeuwen, S.D., Kersten, I., Wildhagen, M.F., van Helvoort, A., 2005. Randomized, double-blind, placebo-controlled crossover study in men with prostate cancer and rising PSA: effectiveness of a dietary supplement. Eur. Urol. 48, 922–930 discussion 930-921.

Shan, X., Li, S., Sun, B., Chen, Q., Sun, J., He, Z., Luo, C., 2020. Ferroptosis-driven nanotherapeutics for cancer treatment. J. Control. Release 319, 322–332.

Shen, Z., Song, J., Yung, B.C., Zhou, Z., Wu, A., Chen, X., 2018. Emerging strategies of cancer therapy based on ferroptosis. Adv. Mater. 30, e1704007.

Shen, B., Dong, C., Ji, J., Xing, M., Zhang, J., 2019. Efficient Fe (III)/Fe (II) cycling triggered by MoO2 in Fenton reaction for the degradation of dye molecules and the reduction of Cr (VI). Chin. Chem. Lett. 30, 2205–2210.

Simunkova, M., Barbierikova, Z., Jomova, K., Hudecova, L., Lauro, P., Alwasel, S.H., Alhazza, I., Rhodes, C.J., Valko, M., 2021. Antioxidant vs. prooxidant properties of the flavonoid, kaempferol, in the presence of Cu(II) Ions: a ROS-scavenging activity, fenton reaction and DNA damage study. Int. J. Mol. Sci. 22, 1619.

Sung, H., Ferlay, J., Siegel, R.L., Laversanne, M., Soerjomataram, I., Jemal, A., Bray, F., 2021. Global cancer statistics 2020: GLOBOCAN estimates of incidence and mortality worldwide for 36 cancers in 185 countries. CA Cancer J. Clin. 71, 209–249.

Tian, L., Zhang, S., Yi, J., Zhu, Z., Cui, L., Decker, E.A., McClements, D.J., 2021. Factors impacting the antioxidant/prooxidant activity of tea polyphenols on lipids and proteins in oil-in-water emulsions. LWT 113024.

Valenzuela, A., Garrido, A., 1994. Biochemical bases of the pharmacological action of the flavonoid silymarin and of its structural isomer silibinin. Biol. Res. 27, 105–112.

Valko, M., Leibfritz, D., Moncol, J., Cronin, M.T., Mazur, M., Telser, J., 2007. Free radicals and antioxidants in normal physiological functions and human disease. Int. J. Biochem. Cell Biol. 39, 44–84.

van Hoogevest, P., Liu, X., Fahr, A., 2011. Drug delivery strategies for poorly water-soluble drugs: the industrial perspective. Exp. Opin. Drug Deliv. 8, 1481–1500.

Wang, J., Wang, X., He, Y., Jia, L., Yang, C.S., Reiter, R.J., Zhang, J., 2019. Antioxidant and pro-oxidant activities of melatonin in the presence of copper and polyphenols in vitro and in vivo. Cells 8, 903.

Xie, Y., Hou, W., Song, X., Yu, Y., Huang, J., Sun, X., Kang, R., Tang, D., 2016. Ferroptosis: process and function. Cell Death Differ. 23, 369–379.

Yan, Z., Wang, Q., Liu, X., Peng, J., Li, Q., Wu, M., Lin, J., 2018. Cationic nanomicelles derived from Pluronic F127 as delivery vehicles of Chinese herbal medicine active components of ursolic acid for colorectal cancer treatment. RSC Adv. 8, 15906–15914.

Yan, Q., Zhang, J., Xing, M., 2020. Cocatalytic Fenton reaction for pollutant control. Cell Rep. Phys. Sci. 1, 100149.

Yordi, E.G., Perez, E.M., Matos, M.J., Villares, E.U., 2012a. Structural alerts for predicting clastogenic activity of pro-oxidant flavonoid compounds: quantitative structure-activity relationship study. J. Biomol. Screen. 17, 216–224.

Yordi, E.G., Pérez, E.M., Matos, M.J., Villares, E.U., 2012b. Antioxidant and pro-oxidant effects of polyphenolic compounds and structure-activity relationship evidence. Nutrition, Well-being Health 2, 23–48.

Zhang, J., Chen, R., Yu, Z., Xue, L., 2017. Superoxide dismutase (SOD) and catalase (CAT) activity assay protocols for *Caenorhabditis elegans*. Bio-Protoc. 7, e2505.

Zhang, J., Li, X., Huang, L., 2020. Anticancer activities of phytoconstituents and their liposomal targeting strategies against tumor cells and the microenvironment. Adv. Drug Deliv. Rev. 154, 245–273.

Zhang, J., Hu, K., Di, L., Wang, P., Liu, Z., Zhang, J., Yue, P., Song, W., Zhang, J., Chen, T., Wang, Z., Zhang, Y., Wang, X., Zhan, C., Cheng, Y.C., Li, X., Li, Q., Fan, J.

Y., Shen, Y., Han, J.Y., Qiao, H., 2021. Traditional herbal medicine and nanomedicine: converging disciplines to improve therapeutic efficacy and human health. Adv. Drug Deliv. Rev. 178, 113964.

Zhao, J., Yang, J., Xie, Y., 2019. Improvement strategies for the oral bioavailability of poorly water-soluble flavonoids: an overview. Int. J. Pharm. 570, 118642.

Zheng, L.F., Dai, F., Zhou, B., Yang, L., Liu, Z.L., 2008. Prooxidant activity of hydroxycinnamic acids on DNA damage in the presence of Cu(II) ions: mechanism and structure-activity relationship. Food Chem. Toxicol. Intern. J. Publ. Br. Industr. Biol. Res. Assoc. 46, 149–156.

Zhou, L., Elias, R.J., 2012. Factors influencing the antioxidant and pro-oxidant activity of polyphenols in oil-in-water emulsions. J. Agric. Food Chem. 60, 2906–2915.

Ziech, D., Franco, R., Pappa, A., Panayiotidis, M.I., 2011. Reactive oxygen species (ROS)–induced genetic and epigenetic alterations in human carcinogenesis. Mutat. Res. 711, 167–173.